Journal of Nuclear Medicine, published on December 31, 2014 as doi:10.2967/jnumed.114.147157

Optoacoustic Imaging of Naphthalocyanine: Potential for contrast enhancement and therapy monitoring.

Running title: Naphthalocyanine in optoacoustic imaging

Nicolas Bézière[1,*], Vasilis Ntziachristos[1]

[1] Institute for Biological and Medical Imaging, Helmholtz Zentrum München and Technische Universität München, D-85764 Neuherberg, Germany.

*Corresponding author: Institute for Biological and Medical Imaging, Helmholtz Zentrum München and Technische Universität München, Building 56, Ingolstädter Landstraße 1, D-85764 Neuherberg, Germany. E-mail: nicolas.beziere@helmholtz-muenchen.de, phone: +49 (0)89 3187 2003 ; fax: +49-(0)89-3187-3008

Competing interests:

V.N. is an equity holder in iThera Medical GmbH.

Word count: 4991.

ABSTRACT

We investigated in vitro and in vivo the optoacoustic responses of a silicon naphthalocyanine (SiNc), considered herein as a reporter molecule for optoacoustic imaging, elucidating its efficiency for optoacoustic (photoacoustic) signal generation and examined the in vivo performance achieved.

Methods

SiNc solutions were prepared using Cremophor E.L. in water and evaluated for light absorbing and photoacoustic contrast generating properties. Photostability and singlet oxygen generation were investigated under pulsed laser illumination and validated using photoabsorbance. HT-29 mice tumor models were used to assess the biodistribution of the compound and its performance as an optoacoustic contrast agent in vivo.

Results

SiNc was found to generate superior optoacoustic signals compared to the commonly used Indocyanine Green (ICG). Multispectral optoacoustic tomography (MSOT) of mouse tumors efficiently resolved the biodistribution of SiNc and the underlying perfusion parameters in vivo. In addition, we demonstrate how light-triggered SiNc reactions with molecular oxygen can be potentially sensed and discuss the relation of these measurements to the biochemical process involved in photothermal treatment.

Conclusion

SiNc appears to be a promising family of contrast agent for optoacoustic imaging. Further development possibilities promise to expand its use in purely contrast generation settings, as well as its photodynamic therapy application.

KEYWORDS

Naphthalocyanine; photodynamic therapy; optoacoustic; photoacoustic; imaging.

INTRODUCTION

Phthalocyanines are strongly colored macrocyclic compounds that represent a class of artificial pigments. Structurally related to porphirin, they share the tetradentate property and can complex metals. Interestingly, metal complexation as well as substitution on the benzene ring of the isoindole allow a red-shift of the absorbance spectra (*1*). The family of molecules of interest herein, Naphthalocyanine, was built using benzoisoindole instead of isoindole blocks and exhibits a sharp and intense absorbance band in the near infra-red region of the spectra (700-900 nm). After light absorption, this family of molecules can react with triplet oxygen to produce singlet oxygen, a highly reactive and cytotoxic oxidant (*2*). Based on photochemical reactions, photochemotherapy has been developed to selectively trigger tissue destruction in cancer (*3*) (*4*) or other pathologies such as psoriasis (*5*). Following the arrival of Photofrin® on the market in 1993 as the first FDA approved synthetic photothermal therapy agent, this class of molecules has been expanded with formulations used for topical and systemic administration modes (*6*). Refining the core structure of phthalocyanines, notably into naphthalocyanines (*7-9*), close derivatives of Photofrin®, alongside adapted delivery vehicles enabled fine tuning of photochemical and pharmacodynamic properties, solved potential solubility issues common in this chemical class (*10*).

Sensing of naphthalocyanines in vivo is important for understanding their bio-distribution in tissues and for determining administered dose and illumination parameters, as underlined by fluorescence imaging studies (*6, 11, 12*). However, classical fluorescence imaging methods cannot resolve depth accurately with good resolution and cannot offer a complete picture of biodistribution, especially considering the generally low quantum yield of naphthalocyanines.

Interestingly, this low quantum yield, combined with a high absorption cross-section, make naphthalocyanines promising dyes for optoacoustic sensing. It was a hypothesis herein that optoacoustic imaging could offer an ideal modality to characterize naphthalocyanines in tissues, due to the high-resolution, three-dimensional imaging through several centimeters provided by optoacoustic methods. Optoacoustic imaging generates optical images by detecting the sound waves produced by photoabsorbers in response to their excitation with light of transient intensity (*13, 14*). Consequently, we investigated the characteristics of silicon 2.3-naphthalocyanine bi(trihexylsilyloxide) (*15-17*) (SiNc, Fig. 1A) in relation to its ability to generate optoacoustic signal. We were particularly interested in identifying the performance of SiNc over the more commonly employed Indocyanine Green (ICG), an organic fluorophore with a high molecular extinction coefficient. ICG is an FDA approved dye with high photoabsorbance but poor stability in vitro and in vivo and extremely rapid excretion (*18-20*). Finally we uncovered how different pulsed laser light energy could trigger the SiNc reaction with oxygen, and monitored the change in optical absorbance in tissue mimicking phantoms.

MATERIALS AND METHODS

Naphthalocyanine and Indocyanine Green Solutions Preparation

Silicon 2.3-naphthalocyanine bi(trihexylsilyloxide) (Sigma-Aldrich) was prepared as an emulsion of 10% Cremophor EL, 1% 1,2-propanediol and 1% dimethylformamide (*16*) (Sigma-Aldrich) in phosphate buffer saline pH 7.4 by sonication. Concentration of the initial preparation was estimated using the absorbance of the solution and using a molar extinction coefficient of 500 000 $M^{-1}cm^{-1}$ at around 40 µM. ICG solutions were prepared using the same emulsion. Reactive oxygen species measurements were performed anthracene-9,10-dipropionic acid (ADPA, Sigma-Aldrich) as a scavenger. An initial solution containing $1.5.10^{-3}$ $mol.L^{-1}$ of ADPA was prepared and used at a 5% dilution in the SiNc solutions for the phantom experiments.

Light Absorbance Measurements

Absorbance of the solutions was recorded on an OceanOptics CUV-UV + USB2000 spectrometer and processed with SpectraSuite (OceanOptics), using a cuvette with a 1 cm light pathway, and recording every 0.1 nm. Absorbance of solutions containing ADPA were recorded in a UV/Visible plate reader SpectraMax $M2^e$ from Molecular Device, using a 96 well plate and recording absorbance every 1 nm.

Optoacoustic System

The experimental multi spectral optoacoustic system employed is custom built and has been previously described extensively (*21*). Supplementary online materials contain an extensive description of the system characteristics. The optoacoustic images were reconstructed using an

interpolated matric model inversion image reconstruction algorithm. Spectral unmixing was applied to detect signals from contrast agents within the samples (*22, 23*).

Phantoms Experiments

Cylindrical phantoms of 2 cm diameter were prepared using a gel made from distilled water, containing Agar (Sigma-Aldrich) for jellification (1.3% w/w) and an intralipid 20% emulsion (Sigma-Aldrich) for light diffusion (6% v/v), resulting in a gel presenting a reduced scattering coefficient of $\mu'^{s} \approx 10$ cm^{-1} and no specific absorbance as to allow precise estimation of light energy deposition. A 3 mm diameter cylindrical inclusion containing the SiNc at an optical density (OD) of 0.5 was placed at the middle of the phantom, alongside a tube containing classical black india ink at OD of 0.3 for intensity measurement references. Tube length was around 4 cm, making for a total volume of solution of around 300 µL.

MSOT imaging was performed at a single position, located approximately in the middle of the phantom. Data acquisition was performed using 10 averages per and at every wavelength between 680 nm and 900 nm in steps of 5 nm resulting in a total acquisition time of around 1.5 min. For photochemical experiments, a complete MSOT spectrum was recorded every 10 minutes for one hour, and pulsed light illumination was maintained between spectral acquisition at 770 nm for SiNc or 800 nm for ICG. After the last time point, the solution was extracted from the MSOT phantom and its absorbance spectrum was recorded in the spectrophotometer described above. Every phantom experiment was performed in triplicates and standard deviations are indicated for the photochemical experiment.

Animal Experiments

Procedures involving animals were conducted in conformity with institutional guidelines, and approved by the government of Upper Bavaria.

Three Female CD-1 nu/nu mice (Charles River Laboratories) were inoculated with 1.5 million HT29 human colon cancer cells in 15 µl BD Matrigel™ (BD Biosciences) subcutaneously between the kidneys and the base of the tail, in the hips region. The cells were cultured in McCoy medium with 1% penicillin/streptomycin and 10% FCS in an atmosphere of 5% CO_2 at 37°C.

For the imaging experiments, 200 µL of a SiNc solution in a 25% Cremophor E.L. emulsion (approx. 2.5 OD) were injected intravenously in the tail vein after anesthesia using 2% isoflurane in oxygen. The anesthesia was maintained at 1.8% isoflurane in oxygen throughout the acquisition. Imaging was performed in the previously described MSOT system using transversal slices at the middle of the tumor, liver and kidney region, at 680, 700, 730, 750, 770, 800, 830, 860 nm illumination wavelength for each position, using 50 averages per wavelength in order to minimize the influence of animal movement in the images. Image acquisition time for each slice was around 1 minute, and laser illumination was not maintained between acquisitions. The animals were sacrificed using cervical dislocation. Figures and calculations are based on a representative animal from the panel used, all three animals displaying similar behavior.

RESULTS

Spectral Measurements

Fig.1 depicts the structure and absorption spectra of SiNc. Fig. 1B shows the absorption spectra obtained from SiNc by optical and optoacoustic measurements from the same solution. Corresponding control measurements were obtained from black India ink and used for reference purposes compensating for possible laser energy fluctuation during the optoacoustic measurements. As shown in Fig 1B, India ink absorbance and optoacoustic spectra correlate closely at all wavelengths. The optical and optoacoustic spectra of SiNc display good correlation above 770 nm. However, in the lower wavelengths, the optoacoustic signal shows an elevated contribution compared to the optical measurements. Two absorption contributions at bands around 690 and 730nm can nevertheless be seen on both the optical and the optoacoustic signal intensity curve. Spectrum measurements obtained from ICG exhibited a similar response (Fig. 1B). SiNc and ICG measurements were repeated multiple times at a SiNc concentrations ranging from 0.1 to 1 OD. In all cases the differences between SiNc spectra determined from the optical and optoacoustic signals were consistent (results not shown). As a negative control, a Cremophor E.L. emulsion devoid of any photoabsorber was measured in similar conditions and did not display light absorption or a bias of the optoacoustic signals compared to optical signals (results not shown). The repeatability of optoacoustic spectra was also examined, to investigate the effects and overall stability of the illumination energy, and is shown in Fig.2A.

SiNc Stability Measurements

As naphthalocyanines' reaction with oxygen is light-triggered, we investigated the behavior of a 0.5 OD SiNc emulsion in a light scattering phantom under pulsed laser illumination in the

optoacoustic imaging system. Fig. 2B shows the evolution of the optoacoustic signal of a SiNc emulsion illuminated by pulsed laser light at 770 nm at energies ranging between 15 mJ and 80 mJ per pulse. At high energy settings (40 and 80 mJ), loss of signal can be seen, resulting in around 70% of the initial value after 1h of illumination. However, using only 15 mJ per pulse, no loss of optoacoustic signal was detected. At 80mJ, a similarly prepared ICG emulsion demonstrated faster photo-bleaching than SiNc, losing 60% of its initial optoacoustic signal after being illuminated for 1h at 800 nm. Transferring the emulsions into a spectrophotometer cuvette to obtain absorbance spectra after optoacoustic signal acquisition confirmed the findings, without any modification of the shape of the spectra (data not shown). Interestingly, at the same absorbance values (0.5 OD), ICG proves around 60% more efficient to provide optoacoustic signal than SiNc at the initial time point (0.27 a.u. compared to 0.16 a.u. respectively). However, given the increased stability of SiNc compared to ICG, its optoacoustic signal strength becomes comparable after 1 h of illumination.

Detection of SiNc in a Murine Subcutaneous Tumor Model

In order to evaluate SiNc in-vivo, we intravenously administered the dye emulsion in mice bearing a 1 cm diameter HT29 tumor. Fig. 3 shows MSOT images obtained from the tumor bearing mouse 5, 15, 30, 45 and 60 min after injection of SiNc. The distribution of SiNc was identified by spectral unmixing (*24*) applied to images obtained at multiple wavelengths. Fig.3A represents the pre-injection hemoglobin oxygenation map and depicts the anatomical features of a subcutaneous xenografted tumor. The main blood vessels (BV) feeding the tumor are indicated, as well as the tumor (Fig. 3A). Fig 3B-F show an accumulation of the contrast agent in the core of the tumor and a clearance of the molecule from the blood vessels surrounding the tumor.

Since spectral unmixing allows for specific detection of SiNc based on its absorption spectra, the data were further processed to reveal the biodistribution of SiNc after i.v. injection. Fig. 4A depicts the optoacoustic spectra derived from SiNc in vivo in the tumor, overlayed with its optoacoustic spectra in a tissue mimicking phantom. The in vitro and in vivo optoacoustic spectra derived from the phantom measurements and in-vivo appear similar to each-other but not identical. The differences could be attributed to the sparse spatial sampling applied in-vivo and possibly spectral alterations due to the wavelength-depended light fluence distribution (*24*). Similarly to the observations in Fig.2, Fig.4A also shows a discrepancy between the absorption spectrum measured by a spectrophotometer (dotted line) and the optoacoustic measurements. While it is unclear why this discrepancy exists, it is also consistent after repeating the measurements multiple times and cannot be attributed to instrument calibration issues. Fig 4B plots the change of SiNc optoacoustic signal strength detected in vivo as a function of time in the tumor region and in blood, from structures identified in Fig. 3A, resulting in a plot of the pharmacokinetic profile of the molecule. Notably, the SiNc optoacoustic signal (Fig. 3B) reaches its peak in the blood a few minutes after injection, while being negligible in the tumor mass, indicating a successful i.v. injection. As confirmed by Fig. 3C, SiNc shows a clear accumulation increase 15 min after injection, with a relative decrease in the blood compartment, pointing at a tumor accumulation of the compound. The respective difference of SiNc optoacoustic signal strength between blood and tumor continues to grow until termination of the experiment (1h, Fig. 3F). At the final time point of acquisition, we could still observe a presence of the SiNc preparation in the liver and kidneys of the animal (Supp. Fig. 1).

Generation of Reactive Oxygen Species in the Optoacoustic System

As pulsed laser illumination at the maximum absorbance wavelength induced an energy-dependent gradual loss of signal in phantoms (Fig. 2B), suggesting a generation of reactive oxygen species, we investigated the underlying physicochemical process of the apparent photobleaching. Fig. 5 shows that the light absorbance of Anthracene-9,10-dipropionic acid (ADPA) recorded in an optical spectrometer, after it was placed in solution with SiNc in a tissue mimicking phantom, decreases after 1h of illumination in the MSOT system at the maximum absorbance wavelength of SiNc (770 nm) with an energy of 40 mJ per 10 ns light pulse at 10 Hz repetition rate. As the singlet oxygen reaction with ADPA causes the loss of absorbance of this oxygen trap, this plot indicates that the chosen illumination settings are sufficient for triggering the reaction between O_2 and SiNc and producing singlet oxygen. Comparatively, similar SiNc – ADPA solutions left for 1h in the dark or under daylight did not show any significant decrease in ADPA absorbance (results not shown), confirming the requirement for laser illumination.

DISCUSSION

We investigated the suitability of silicon 2.3-naphthalocyanine bi(trihexylsilyloxide) (SiNc) to generate optoacoustic signals and then employed MSOT to monitor SiNc characteristics in vitro and in vivo. SiNc (*16, 17*) is an interesting dye for optoacoustic studies as it displays sharp absorption in the near-infrared (peak at 770 nm), a spectral region where light can penetrate several centimeters within tissues. A sharp absorbance change is beneficial for the identification of photoabsorbers, since they can then be resolved by wavelength scanning and differentiated from the spectral signatures of other (*25*). In the particular case of SiNc, the absorbance change between 770 nm and 800 nm is remarkably steeper than with ICG, highlighting a beneficial feature of SiNc as a contrast agent for optoacoustic imaging. Measurements of the SiNc and ICG spectra showed a reproducible discrepancy between optical and optoacoustic observations in the 700-750nm wavelength region (Fig. 1B). The spectra were acquired on the exact same solution, confirming that the SiNc was still in a monomeric state favored by the bulky axial silicon ligand, characterized by a sharp absorbance band at 770nm (*16*).

This result is unexpected. While methodology errors are a first suspect, there is no justification of system bias in these studies. Indian ink, a stable photoabsorber presenting a characteristically flat absorbance spectra, was incorporated alongside the SiNc and ICG measurements to control for system bias but did not exhibit any discrepancy in shorter wavelengths; excluding system and experimental faults.

Possible explanations can include influence of the silicon ligand inside of the complex dampening the optoacoustic effect of the π-π^* transition resulting from the light absorption at 770 nm, leading to a lower apparent ultrasonic energy emitted and thus a flattened spectrum; or a

comparatively much bigger influence of the small absorption peak located between 680 and 750 nm with higher energy pressure waves being emitted. Several other physical parameters that could have an influence on the shape have been investigated, in particular the scanning direction (longer to shorter or shorter to longer wavelengths), SiNc concentration and influence of Cremophor E.L. without tangible results. Only when changing the amount of energy used we could see a modification of the spectra which confirms a power related mechanisms (Fig. 2A). Light energy was found to also impact the stability of the SiNc, with a threshold for the decomposition located between 15 and 40 mJ per pulse (Fig. 2B). Remarkably, even though the loss of signal due to light energy deposited on the sample was noticeable, it remained less marked than ICG at comparable concentration and thus justified the use of SiNc as a contrast agent able to provide a distinctive signature in the MSOT system with a 2.5 times higher molar extinction coefficient as ICG and less photobleaching (500 000 $M^{-1}cm^{-1}$ compared to 200 000 $M^{-1}cm^{-1}$ respectively). In terms of optoacoustic signal strength, even though ICG initially provides around 60% more signal than SiNc using the same optical density for the solution, the difference quickly diminishes and becomes negligible after 1h of experiment, making SiNc almost twice as efficient as ICG to provide optoacoustic signal per mole. This indicates that specific preparations of SiNc, for example liposomal or micellar, could overtake ICG as the organic contrast agent of choice for optoacoustic imaging, since providing a more reliable contrast enhancement throughout the experiment duration in longitudinal studies is crucial, especially when comparing intensities between different time points.

As the spectral characteristics of SiNc were proven interesting for optoacoustic contrast in vitro, identification of the compound in living animals was investigated after intra vascular injection of an emulsion in a mouse bearing a subcutaneous tumor. Since emulsions of Cremophor E.L. are

known to increase the circulation half-life time of the formulated compounds, we monitored the accumulation of the probe in the tumor and its clearance from the blood flow. Interestingly, the signal coming from SiNc was still easy to identify even though the amount injected was low, and an accumulation in the middle of the tumor, corresponding to a vascularized compartment, could be seen. Since blood vessels in the vicinity of the tumor were readily accessible, monitoring the disappearance of the probe from the blood flow was also possible. Simultaneously, MSOT provided access to real time monitoring of the accumulation of the SiNc in the tumor compartment unavailable volumetrically by other means. The optoacoustic signal from the SiNc in vivo was similar to the one obtained in vitro, with an intense signal coming from the lower wavelength and a sharp drop between 770 and 800 nm, making the SiNc signal easily identifiable.

Since the phthalocyanine-like complexes are known to display photodynamic reactions under high light energy, we hypothesized that this could explain at least in part the decrease in light absorbance of the solution after pulsed laser light exposition. The use of a reactive oxygen species (ROS) scavenger such as ADPA allows observation of the phenomenon by visible absorbance measurements after reaction with ROS, a behavior that could be clearly seen in our experimental conditions (Fig. 5) suggesting that 40 mJ energy per pulse was sufficient to trigger a photochemotherapy like mechanism, which we could not see in lower energy conditions. In our scattering phantom setup, that results in a total of approximately 100 $J.cm^{-2}$ after 1 h of experiment. This data should be compared to the classical way of generating ROS species when using phthalocyanine derivative with a continuous wave laser, typically using 100 to 400 $J.cm^{-2}$ (*16*). It is however not straightforward to compare pulsed and continuous laser energy deposition, and further experiments will be performed to provide quantitative data using pulsed

laser energy. In vivo, and under our parameters, the light fluence condition render the estimation of the amount of light received by the tumor difficult, so it is currently not possible to anticipate whether or not continuous illumination during the experiment would have proven to be sufficient to trigger the photochemotherapy effect on site.

SiNc proves to be a promising example of the phthalocyanine family to be used as a contrast agent for MSOT imaging. Its spectral properties, increased stability and increased optoacoustic signal generation per mole compared to ICG should push it toward the front scene of this new imaging modality purely for contrast generation at even lower light energy settings. Additionally, when taking into account another property of phthalocyanines, namely light-triggered ROS species generation, this family of polycyclic compounds exhibits promising application in the new field of theranostics, in this particular case a dual imaging – photochemotherapy approach. MSOT was able to monitor this photochemical reaction between SiNc and oxygen in vitro, and provided access to the power dependent generation of ROS in real time. From then on, two possibilities of further development of naphthalocyanine exist for use in optoacoustic: firstly, by using non ROS-generating derivatives, a new organic "gold standard" contrast agent could become accessible. Secondly, by tailoring specifically the naphthalocyanine to capitalize on energy-triggered ROS production, a new approach of theranostic with real-time monitoring is made available with direct applicability in various conditions, in particular for photochemical destruction of cancer cells. Naphthalocyanines and related structures have seen a large number of molecules synthesized(*6*), and a different screening approach based on optoacoustic-driven parameters could potentially benefit this new application field. It is anticipated that MSOT contrast agents will become a prominent research field in the coming years, and make use of the dual nature of the modality to exhibit unique theranostic properties and applications.

CONCLUSION

As optoacoustic imaging confirms its place as a pivotal modality in modern imaging techniques, the need for identification of efficient contrast generating agents becomes predominant. Classically used contrast agents such as ICG and gold nanorods have significant drawbacks, be it instability or poor body tolerance. By investigating the potential of SiNc for optoacoustic imaging, we uncovered the significant benefits of the high molar extinction coefficient and sharp absorbance peak and its ease in identifying its distribution in vivo in a tumor model. Most notably, we showed that MSOT of SiNc was able to trigger the generation of reactive oxygen species at the highest energy settings, effectively enabling photodynamic therapy. Additionally, MSOT was able to monitor the kinetics of this reaction by estimating the amount of naphthalocyanine present in the image. We believe this will open the widow to real-time monitoring of the biodistribution of such an agent, while simultaneously enabling evaluation of its pharmacological activity and efficiency, bringing MSOT firmly into the theranostic field.

AUTHOR CONTRIBUTIONS

N.B. designed and performed research and analyzed the data. N.B and V.N. wrote the manuscript.

ACKNOWLEDGMENTS

The authors would like to thank the Deutsche Forschungsgemeinsaft (DFG), Sonderforschungsbereich-824 (SFB-824), subproject A1 and the ERC Advanced Grant (233161) Next Generation in-vivo imaging platform for post-genome biology and medicine MSOT for their financial support.

REFERENCES

1. Roeder B, Naether D, Lewald T, Braune M, Nowak C, Freyer W. Photophysical properties and photodynamic activity in vivo of some tetrapyrroles. *Biophys Chem.* 1990;35:303-312.

2. Dougherty H, Gomer CJ, Jori G, et al. Photodynamic therapy. *J Natl Cancer Inst.* 1998;90:889-905.

3. Brown SB, Brown EA, Walker I. The present and future role of photodynamic therapy in cancer treatment. *Lancet Oncol.* 2004;5:497-508.

4. Davids LM, Kleemann B. Combating melanoma: the use of photodynamic therapy as a novel, adjuvant therapeutic tool. *Cancer Treat Rev.* 2011;37:465-475.

5. Tandon YK, Yang MF, Baron ED. Role of photodynamic therapy in psoriasis: a brief review. *Photodermatol Photoimmunol Photomed.* 2008;24:222-230.

6. Josefsen LB, Boyle RW. Photodynamic therapy and the development of metal-based photosensitisers. *Met-Based Drugs.* 2008;2008:276109-276109.

7. Cuomo V, Jori G, Rihter B, Kenney ME, Rodgers MA. Liposome-delivered Si(IV)-naphthalocyanine as a photodynamic sensitiser for experimental tumours: pharmacokinetic and phototherapeutic studies. *Br J Cancer.* 1990;62:966-970.

8. Margaron P, Langlois R, van Lier JE, Gaspard S. Photodynamic properties of naphthosulfobenzoporphyrazines, novel asymmetric, amphiphilic phthalocyanine derivatives. *J Photochem Photobiol B.* 1992;14:187-199.

9. Sessler JL, Magda DJ. Biomedical applications of texaphyrins. *Free Radical Biology and Medicine.* 2006;41:S8-S8.

10. Wohrle D, Shopova M, Muller S, Milev AD, Mantareva VN, Krastev KK. Liposome-delivered Zn(II)-2,3-naphthalocyanines as potential sensitizers for PDT: synthesis, photochemical, pharmacokinetic and phototherapeutic studies. *J Photochem Photobiol B.* 1993;21:155-165.

11. Lv F, He X, Wu L, Liu T. Lactose substituted zinc phthalocyanine: a near infrared fluorescence imaging probe for liver cancer targeting. *Bioorg Med Chem Lett.* 2013;23:1878-1882.

12. Witjes MJ, Speelman OC, Nikkels PG, et al. In vivo fluorescence kinetics and localisation of aluminum phthalocyanine disulphonate in an autologous tumour model. *Br J Cancer.* 1996;73:573-580.

13. Ntziachristos V. Going deeper than microscopy: the optical imaging frontier in biology. *Nat Methods.* 2010;7:603-614.

14. Luke GP, Nam SY, Emelianov SY. Optical wavelength selection for improved spectroscopic photoacoustic imaging. *Photoacoustics.* 2013;1:36-42.

15. Wheeler BL, Nagasubramanian G, Bard AJ, Schechtman LA, Kenney ME. A silicon phthalocyanine and a silicon naphthalocyanine: synthesis, electrochemistry, and electrogenerated chemiluminescence. *J Am Chem Soc.* 1984;106:7404-7410.

16. Brasseur N, Nguyen TL, Langlois R, et al. Synthesis and photodynamic activities of silicon 2,3-naphthalocyanine derivatives. *J Med Chem.* 1994;37:415-420.

17. Brasseur N, Ouellet R, Lewis K, Potter WR, van Lier JE. Photodynamic activities and skin photosensitivity of the bis(dimethylthexylsiloxy)silicon 2,3-naphthalocyanine in mice. *Photochem Photobiol.* 1995;62:1058-1065.

18. Zhong J, Yang S, Zheng X, Zhou T, Xing D. In vivo photoacoustic therapy with cancer-targeted indocyanine green-containing nanoparticles. *Nanomedicine (Lond).* 2013;8:903-919.

19. Buehler A, Herzog E, Razansky D, Ntziachristos V. Video rate optoacoustic tomography of mouse kidney perfusion. *Opt Lett.* 2010;35:2475-2477.

20. Herzog E, Taruttis A, Beziere N, Lutich AA, Razansky D, Ntziachristos V. Optical imaging of cancer heterogeneity with multispectral optoacoustic tomography. *Radiology.* 2012;263:461-468.

21. Ma R, Taruttis A, Ntziachristos V, Razansky D. Multispectral optoacoustic tomography (MSOT) scanner for whole-body small animal imaging. *Optics Express.* 2009;17:21414-21426.

22. Buehler A, Rosenthal A, Jetzfellner T, Dima A, Razansky D, Ntziachristos V. Model-based optoacoustic inversions with incomplete projection data. *Medical Physics.* 2011;38:1694-1704.

23. Rosenthal A, Razansky D, Ntziachristos V. Fast semi-analytical model-based acoustic inversion for quantitative optoacoustic tomography. *IEEE Trans Med Imaging.* 2010;29:1275-1285.

24. Tzoumas S, Deliolanis NC, Morscher S, Ntziachristos V. Unmixing molecular agents from absorbing tissue in multispectral optoacoustic tomography. *IEEE Trans Med Imaging.* 2014;33:48-60.

25. Ntziachristos V, Razansky D. Molecular imaging by means of multispectral optoacoustic tomography (MSOT). *Chem Rev.* 2010;110:2783-2794.

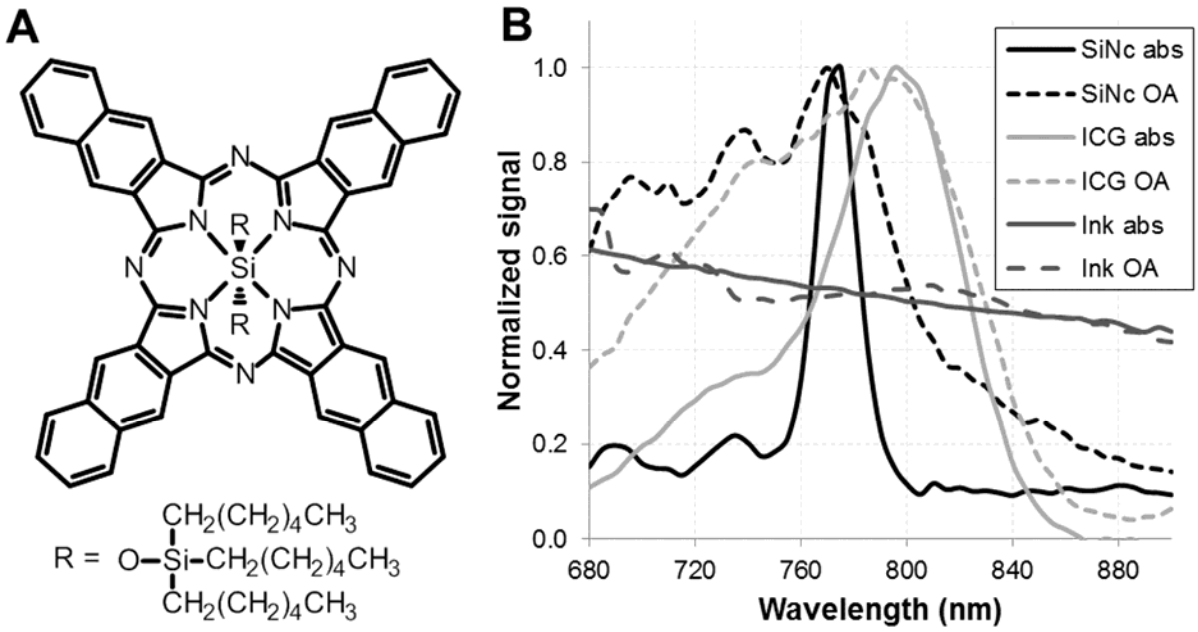

Figure 1: Structure of silicon 2,3-naphthalocyanine bis(trihexylsilyloxide) (SiNc) and its light absorption and optoacoustic spectra compared to indocyanine green. A Structure of SiNc. **B** Overlay of the normalized light absorption spectra (abs) and optoacoustic signal (OA) obtained in the near infra red wavelength range of a naphthalocyanine emulsion (SiNc, black), an indocyanine green solution (ICG, light grey) and India ink (Ink, dark grey). Solutions were prepared with an optical density of 0.5 for ICG and SiNc and 0.3 for India ink.

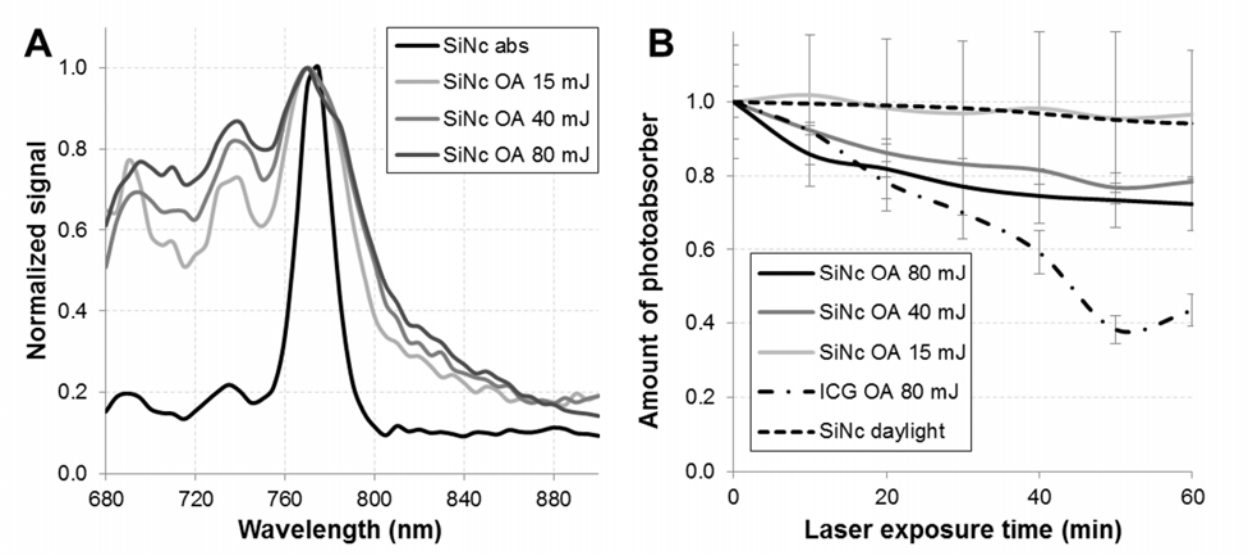

Figure 2: Influence of laser light on a solution of 2,3-naphthalocyanine bis(trihexylsilyloxide) (SiNc). A Normalized optoacoustic signal obtained in the NIR range for the SiNc solution using an average power of 15 mJ (OA 15 mJ); 40 mJ (OA 40 mJ) and 80 mJ (OA 80 mJ) laser energy per 10 ns pulse with the normalized light absorption spectrum (abs) of the same solution for reference. **B** Relative amount through time of SiNc detected in the optoacoustic system (OA) under constant laser pulses exposition at different energy steps (15; 40 and 80 mJ), using the light absorbance of a similar solution left under day light (daylight) as well as indocyanine green (ICG) decay under 80 mJ pulsed laser light as detected in the optoacoutic system for comparison.

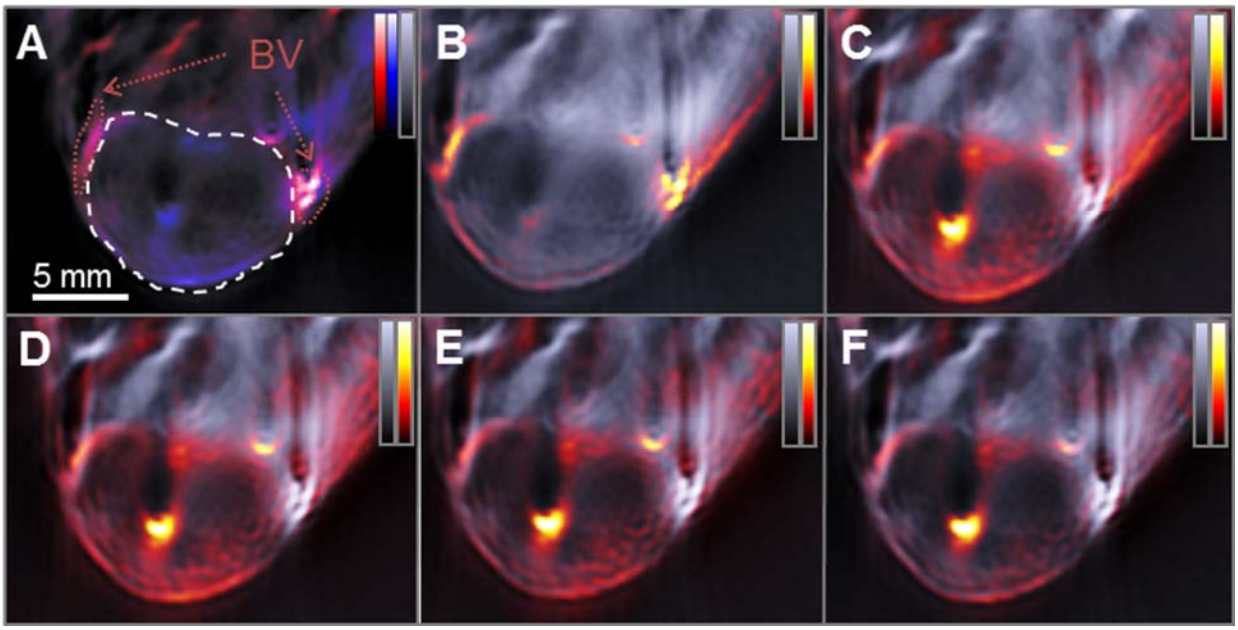

Figure 3: Multispectral optoacoustic tomography of a living mouse bearing an HT29 tumor on its back before and after intra-vascular injection of SiNc. The optoacoustic signal intensity obtained using a 800nm illumination wavelength (grey scale) is used as background in every frame, and overlayed with the signal identified as coming from the SiNc (hot scale). **A** Pre-injection image, indicating the tumor (dashed white circle) and surrounding blood vessels (BV, dotted red circles), overlayed with deoxygenated (blue scale) and oxygenated (red scale) hemoglobin signal. **B-F** Images acquired after 5 (B), 15 (C), 30 (D), 45 (E) and 60 (F) minutes after intra venous injection of SiNc in the tumor bearing animal.

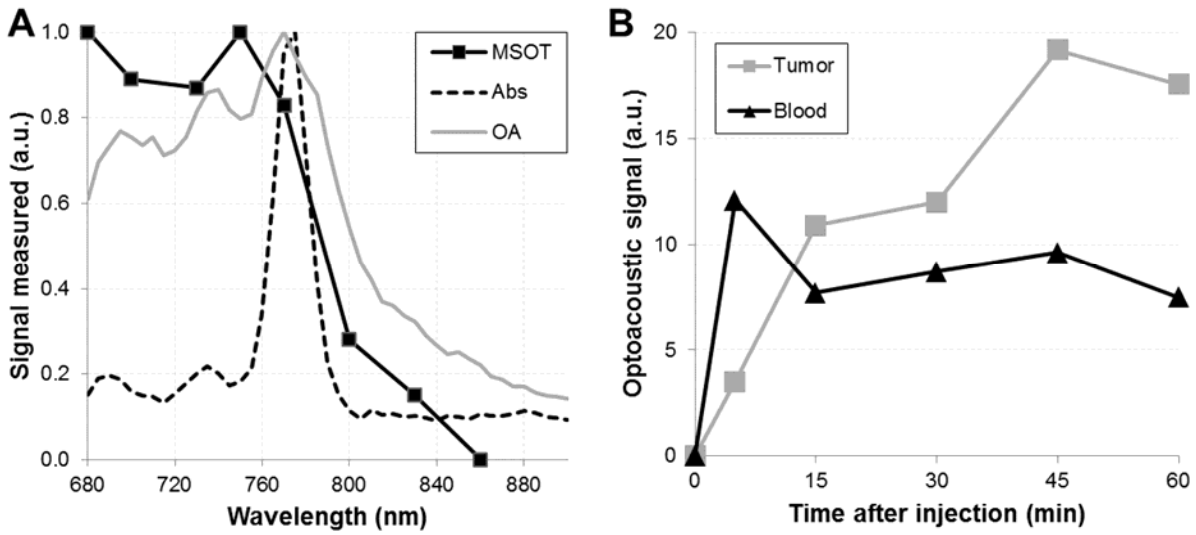

Figure 4: Spectral analysis of the multispectral optoacoustic tomography data acquired after injection of silicon naphthalocyanine (SiNc) in a tumour bearing mouse. A Light absorbance spectrum of the naphthalocyanine solution (Abs, dashed black line) and optoacoustic signal strength obtained at different wavelength obtained in a phantom (OA, grey line) and 1 hour after intra-vascular injection in a tumor bearing mouse using principal component analysis of the acquired multispectral optoacoustic tomography data (MSOT, black line). **B** Maximum optoacoustic signal obtained from SiNc after identification of its spectrum using principal component analysis in the blood compartement (black line) and the tumor area (grey line) after intra-vascular injection in a HT29 tumor mouse model.

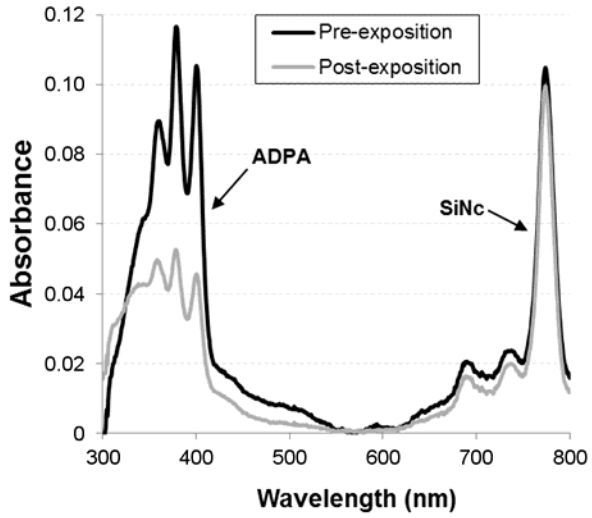

Figure 5: Evolution of the light absorption spectrum of a silicon naphthalocyanine (SiNc) and anthracene-9,10-dipropionic acid (ADPA) solution under pulsed laser light. UV-visible light absorption spectra of a mixture of (ADPA, maximum absorbance located around 350 nm) and SiNc (absorption peak at 770 nm) pre-exposition (black line) and post-exposition (grey line) to pulsed 770 nm laser light for 1 h using 40 mJ per pulse.

The Journal of NUCLEAR MEDICINE

Optoacoustic Imaging of Naphthalocyanine: Potential for contrast enhancement and therapy monitoring

Nicolas Beziere and Vasilis Ntziachristos

J Nucl Med.
Published online: December 31, 2014.
Doi: 10.2967/jnumed.114.147157

The Journal of Nuclear Medicine is published monthly.
SNMMI | Society of Nuclear Medicine and Molecular Imaging
1850 Samuel Morse Drive, Reston, VA 20190.
(Print ISSN: 0161-5505, Online ISSN: 2159-662X)

SNMMI SOCIETY OF NUCLEAR MEDICINE AND MOLECULAR IMAGING